JOURNAL OF CATALYSIS 107, 195–200 (1987)

Surface Acidity and Basicity of TiO_2–ZrO_2–V_2O_5: Dehydrogenation and Isomerization of Cyclohexane

REY-CHEIN CHANG* AND IKAI WANG

Department of Chemical Engineering, National Tsing Hua University, Hsinchu, Taiwan, Republic of China

Received January 14, 1987; revised April 14, 1987

The ternary oxides, TiO_2–ZrO_2–V_2O_5 with an equal molar ratio of TiO_2 and ZrO_2, were characterized by the dehydrogenation and isomerization reactions of cyclohexane. The effects of V_2O_5 molar ratio on the acidic and basic properties, crystal structure, V=O species, and the reaction activities were investigated. The maximum activities of both reactions were observed at the V_2O_5 molar ratio of 0.1 when the calcination temperature was 600°C. That correlated well with surface acidic sites. The crystalline separation of ternary oxides was observed at a V_2O_5 molar ratio higher than 0.25. The reaction of dehydrogenation was retarded by K_2O but not significantly by B_2O_3, which indicates that the acidic sites play an important role in dehydrogenation reaction. A stepwise bifunctional mechanism was proposed.

INTRODUCTION

It has been recognized for some time that catalysts for dehydrogenation are divided into two groups of metal catalysts and oxide catalysts according to their active sites and kinetics (*1, 2*). Among the reforming reactions of petroleum fraction catalyzed by metals and metal oxides, dehydrogenation of cyclohexane to form benzene is one of the easiest reactions to be studied. A degradation mechanism was proposed by Block (*3*) for the dehydrogenation of cyclohexane and has been employed by several workers (*4–6*). The catalytic activity of Pt/Al_2O_3 for the dehydrogenation of cyclohexane has been explained by a single-center mechanism (*7, 8*), while oxide catalysts usually proceed by a doublet mechanism. Richardson and Rossington (*9*) have suggested that the catalytic activities of oxide catalysts are determined by the 3*d* electron configuration of the metal ion.

A doublet acid–base bifunctional mechanism was proposed by Wang *et al.* (*10, 11*) and Wu *et al.* (*12*) to explain the relationship between the surface properties and the activities of the catalysts for ethylbenzene and ethylcyclohexane dehydrogenation. Wang (*11*) pointed out that the dehydrogenation of saturated rings required a stronger surface acidity compared to that of aromatic side chains. Ai (*13*) reported that incorporation of V_2O_5 into TiO_2 could stabilize the acidic sites.

This work is intended to characterize the intrinsic catalytic properties of ternary oxides, TiO_2–ZrO_2–V_2O_5, via the dehydrogenation and isomerization of cyclohexane. The incentive, of course, is to tailor individual supports explicitly to the feedstocks and the desired products. Ensuing publications will discuss hydrogenation and hydrodesulfurization, catalyzed by the reduced and sulfided Co–Mo/TiO_2–ZrO_2–V_2O_5.

EXPERIMENTAL

TiO_2–ZrO_2–V_2O_5 catalysts with equal molar ratios of TiO_2 and ZrO_2 were prepared by coprecipitation of a solution of $TiCl_4$, $ZrCl_4$, and VCl_3 in anhydrous alcohol with aqueous ammonia (33%). The precipitates were aged at room temperature for 1 day, washed with distilled water until no chloride ions were detected by the addition of $AgNO_3$ to the filtrates, dried at 110°C for

* Present address: CTCI/Catalyst Research Center.

0021-9517/87 $3.00

6 hr, and then calcined in air for 2 hr at a rate of 1°C/min up to a series of temperatures.

The acid strength and acid amounts of catalysts were measured by titrating the powder suspended in benzene with 0.1 *N* *N*-butylamine. Dicinnamalacetone ($pK_a \leq -3.0$) was used as an indicator. Titration of dark-colored solids, which had higher V_2O_5 molar ratios, was carried out by adding a small amount of a white solid acid (*14*). The acidic and basic properties of the catalysts were determined via *N*-butylamine or acetic acid adsorption as was done by Wang *et al.* (*10, 11*).

X-ray diffraction (XRD) patterns of catalysts were obtained using Toshiba X-ray diffractometer at $\lambda \sim 1.54$ Å over the range of $2\theta = 4$–$60°$ for the powdered samples. The intensities of V=O and V–O–V adsorption bands of catalysts were observed using a Hitachi Model 270-30 infrared spectrometer over the range of 400–1200 cm^{-1}.

The kinetics of dehydrogenation and isomerization were studied via a flow method as was done by Wang *et al.* (*10, 11*). A schematic diagram of the system is shown in Fig. 1. The dehydrogenation of cyclohexane over TiO_2–ZrO_2–V_2O_5 gives benzene as the dehydrogenation product, and both methylcyclopentane and open-chain compounds through an acid-catalyzed carbonium ion mechanism as the isomerization products. To avoid the competition of a secondary reaction, the benzene

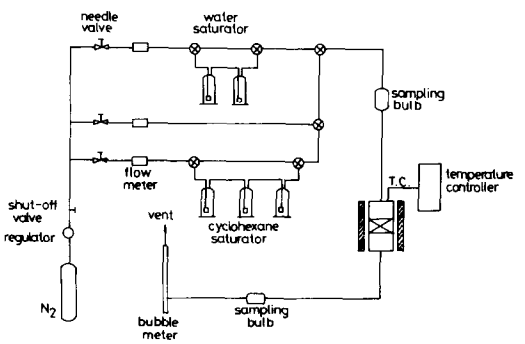

FIG. 1. The flow diagram of a reaction system.

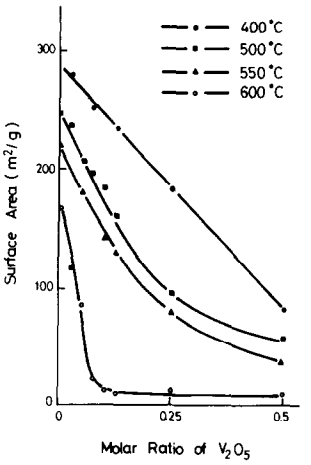

FIG. 2. Surface area of TiO_2–ZrO_2–V_2O_5 at various V_2O_5 molar ratios and calcination temperatures.

yield was limited to the range of 3–15%. The low conversion of cyclohexane ensures that the reaction network may be treated as a parallel first-order reaction for both the dehydrogenation and the isomerization. The α-test method (*15, 16*) was used to determine kinetic data. An alumina (SA 208 m^2/g) was chosen as the reference catalyst to compare the catalytic activities of dehydrogenation and isomerization at 540°C.

RESULTS AND DISCUSSIONS

Data on the surface area vs V_2O_5 molar ratio at a series of calcination temperatures are shown in Fig. 2. Below 550°C, the surface area of TiO_2–ZrO_2–V_2O_5 decreases linearly with the increasing V_2O_5 molar ratios. At 600°C, the surface area of TiO_2–ZrO_2–V_2O_5 sharply decreases as the V_2O_5 molar ratio increases to 0.1, and then levels off as V_2O_5 molar ratio further increases. The significant decrease in surface area at a V_2O_5 molar ratio up to 0.1 is believed to relate to the change of the pore size distribution of TiO_2–ZrO_2–V_2O_5. The pore size distribution of the catalysts at 600°C increases with the increasing V_2O_5 molar ratio, as shown in Fig. 3. The range of mesopore diameter at 30–500 Å has been agreed to contribute mainly on the surface

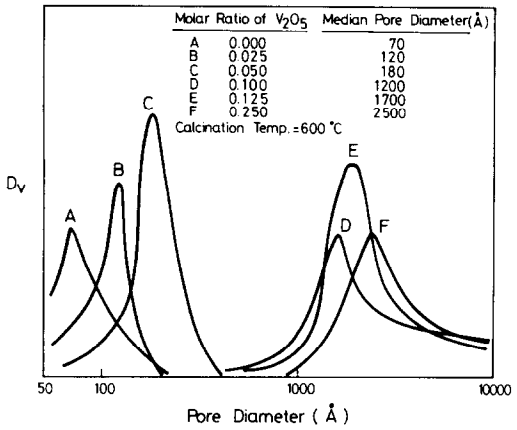

FIG. 3. Pore size distribution of TiO_2–ZrO_2–V_2O_5 at 600°C.

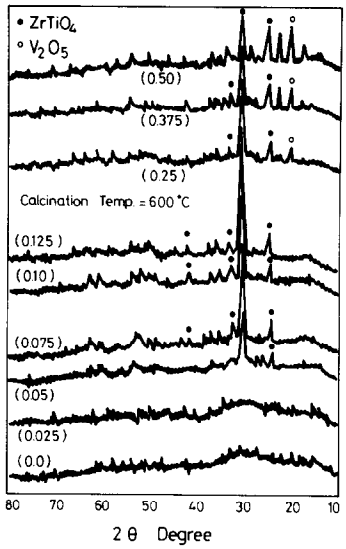

FIG. 5. X-ray diffraction pattern of TiO_2–ZrO_2–V_2O_5 at various V_2O_5 molar ratios.

area (*17*). Therefore, the abrupt switch from mesopore to macropore as V_2O_5 molar ratio increases from 0.05 to 0.1 could explain the significant decrease in surface area found in Fig. 2.

Both the acidic and the basic site densities, defined as the amount of acid (or base) per unit surface area of TiO_2–ZrO_2–V_2O_5, peak at a V_2O_5 molar ratio of 0.1, as shown in Fig. 4. They both have a volcano shape. The results are different from those of TiO_2–V_2O_5 binary oxide (*14*); the acidic sites of TiO_2–V_2O_5 increase steadily with the increasing V_2O_5 content.

In order to unveil the novel phenomena

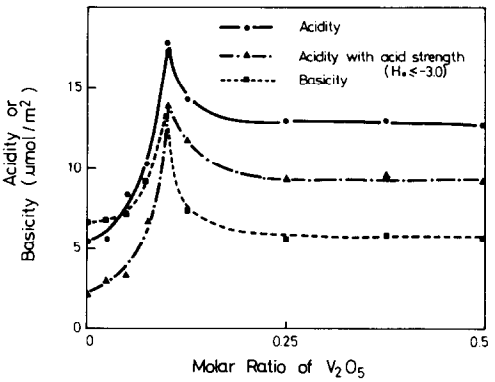

FIG. 4. Acidity and basicity of TiO_2–ZrO_2–V_2O_5 at various V_2O_5 molar ratios.

described above, we studied the crystal structure and functional groups of those catalysts. The XRD patterns of catalysts with various V_2O_5 molar ratios and calcination temperatures are shown in Figs. 5 and 6, respectively. For catalysts calcined at 600°C, crystalline $ZrTiO_4$, identified by the peaks of 2θ = 24.7(m), 30.6(vs), 32.9(m), and 42.2(w) (*18*), begins to show up at a V_2O_5 molar ratio of 0.05, reaches a maximum at 0.1, and decreases again as the V_2O_5 molar ratio further increases. Figure 6 also indicates that $TiO_2ZrO_2V_2O_5$ (1/1/0.1) shows a maximum crystallinity of $ZrTiO_4$ at 600°C. Wang (*12*) has found that with TiO_2 ZrO_2 (1/1) the crystalline $ZrTiO_4$ appeared at 650°C, and reached a maximum at 900°C. Therefore, the incorporation of V_2O_5 into TiO_2ZrO_2 (1/1) not only induces the formation of crystalline $ZrTiO_4$ at a lower temperature, but also enhances the crystalline intensity. The peaked acidity and basicity at V_2O_5 of 0.1 correlate with the maximum intensity of crystalline $ZrTiO_4$. This shows a mutual interaction between V_2O_5 and $ZrTiO_4$. Crystalline V_2O_5 of catalysts, identified by the peaks of 2θ = 15.4(m),

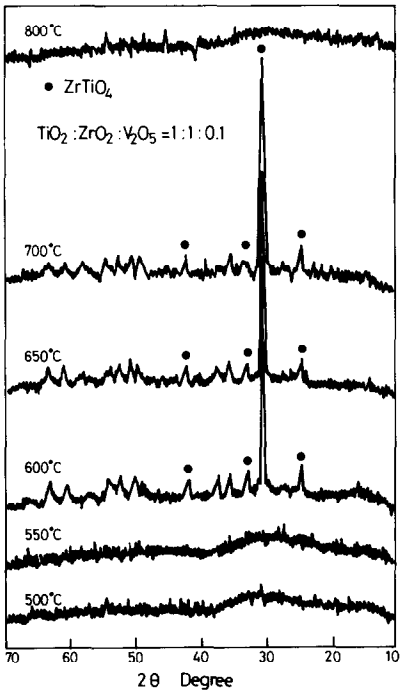

FIG. 6. X-ray diffraction pattern of $TiO_2ZrO_2V_2O_5$ (1/1/0.1) at various calcination temperatures.

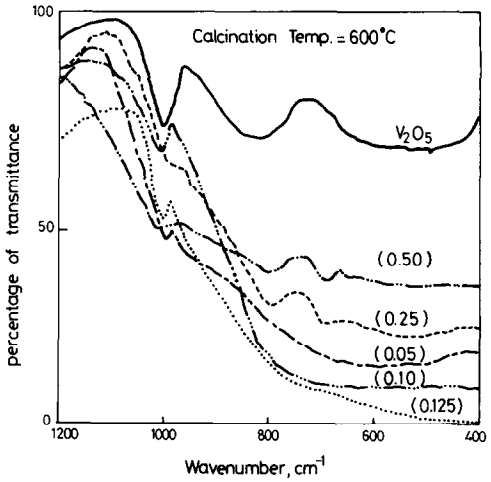

FIG. 7. Infrared spectrum of TiO_2–ZrO_2–V_2O_5 at various V_2O_5 molar ratios.

20.2(vs), 21.8(m), 26.2(m) (*18*), gradually appears as V_2O_5 molar ratio is above 0.25.

Figure 7 shows infrared spectra of catalysts at various V_2O_5 molar ratios. An absorption band was observed at 1020–1040 cm^{-1}, which has been assigned to the V=O stretching vibration (*20, 21*). This absorption band becomes stronger with an increasing V_2O_5 molar ratio, reaches a maximum at 0.1, and then decreases as the V_2O_5 molar ratio further increases. Inomata *et al.* (*22*) concluded that a V=O species of V_2O_5–TiO_2 was selectively exposed on the surface. Thus, we speculate that the appearance of a V=O species due to the presence of V_2O_5 is the major factor affecting the formation of crystalline $ZrTiO_4$. In addition, as the V=O stretching band further decreases, the V–O–V symmetrical and unsymmetrical stretching bands, observed at 800 and 700 cm^{-1}, respectively, begin to appear at a V_2O_5 molar ratio of 0.25, as shown in Fig. 7. This together with the XRD result that crystalline V_2O_5 begins to appear at the V_2O_5 molar ratio of 0.25 indicates that a higher V_2O_5 molar ratio causes a phase separation of V_2O_5 and $ZrTiO_4$. Higher acidity of these ternary oxides, shown in Fig. 4, is due to the separation of V_2O_5 (*14*).

Figure 8 shows that the activity for the

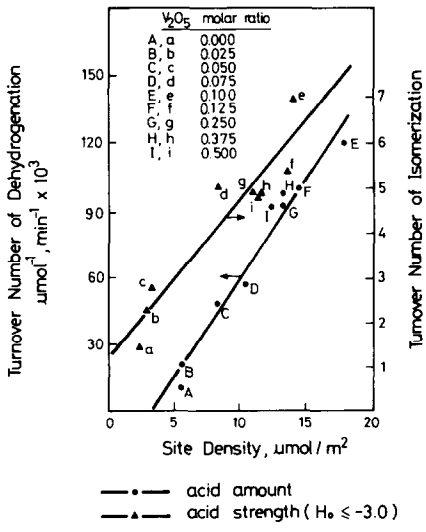

FIG. 8. Correlation of the activities of cyclohexane dehydrogenation and isomerization with acidic site densities.

dehydrogenation correlates well with the acid sites (*N*-butylamine). This agrees with Ferreira (*8*) that the dehydrogenation of cyclohexane over supported metal catalysts depended on the coordination of acidic sites with hydrides. TiO_2ZrO_2 (1/1) binary oxide is impractical as a catalyst for dehydrogenation of cyclohexane. However, the ternary oxide, TiO_2–ZrO_2–V_2O_5, is more effective, and the maximum activity is observed at a V_2O_5 molar ratio of 0.1. We speculate that the dehydrogenation of cyclohexane over TiO_2–ZrO_2–V_2O_5 catalysts proceeds by a stepwise two-center mechanism, as shown in Fig. 9. The abstraction of one hydride ion by acidic sites to form the cyclohexyl carbenium ion intermediate appears to be the rate-determining step, whereas the removal of one proton by basic sites is a fast step. The correlation between the skeletal isomerization of hydrocarbons and the concentration of stronger acid sites of catalsyts has been generally accepted (*23, 24*). Pines and Haag (*25*) indicated that the isomerization of cyclohexene to methylcyclopentane over alumina was due to Brønsted acid sites on the surface. Since the activity for isomerization, shown in Fig. 8, is correlated with the acidic sites ($H_0 \leq -3.0$) of the TiO_2–ZrO_2–V_2O_5 catalysts, we conclude that the stronger acidic sites ($H_0 \leq -3.0$) are the major factors affecting the activity for cyclohexane isomerization.

In order to elucidate the roles of acidic and basic sites played in the dehydrogenation of cyclohexane, K_2O and B_2O_3 was introduced by the incipient wetness impregnation to $TiO_2ZrO_2V_2O_5$ (1/1/0.1). Since the surface area of these catalysts varies little due to the small quantities of K_2O or B_2O_3 (0.5–2.0 wt%), the activity is expressed as the ratio of rate constant of the doped to $TiO_2ZrO_2V_2O_5$ (1/1/0.1). Figure 10 shows that increasing the K_2O content in the catalysts reduces both the activity and the adsorbed *N*-butylamine, but that it has a negligible effect on the amount of adsorbed acetic acid. On the other hand, increasing the B_2O_3 content causes a significant drop in the concentration of basic sites. The slight decrease in activity is due to mild poisoning of acidic sites, as shown in Fig. 11. Based on these results as well as on the good correlation between the activity of dehydrogenation and acidic sites (*N*-butylamine), we conclude that the acidic sites of TiO_2–ZrO_2–V_2O_5 catalysts play the most important role in the dehydrogenation of cyclohexane, as described in Fig. 9.

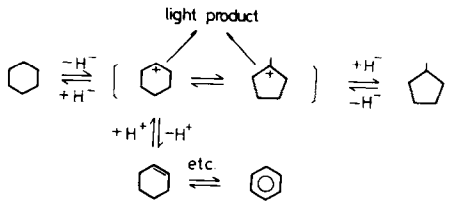

FIG. 9. The mechanism of cyclohexane dehydrogenation and isomerization over TiO_2–ZrO_2–V_2O_5.

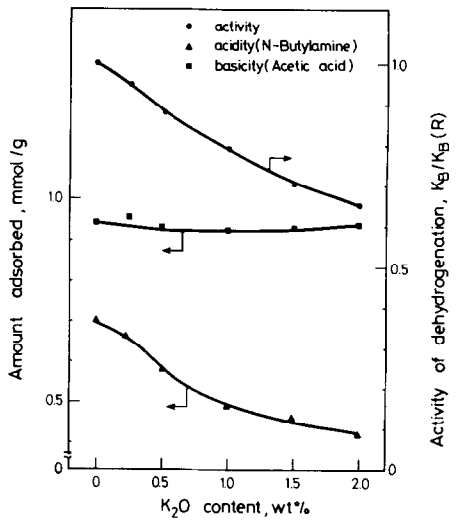

FIG. 10. Effect of doping with K_2O on the activity of dehydrogenation and an adsorbed amount of *N*-butylamine and acetic acid.

CONCLUSIONS

The ternary oxides, TiO_2–ZrO_2–V_2O_5 with an equal molar ratio of TiO_2 and ZrO_2, were characterized by the dehydrogenation

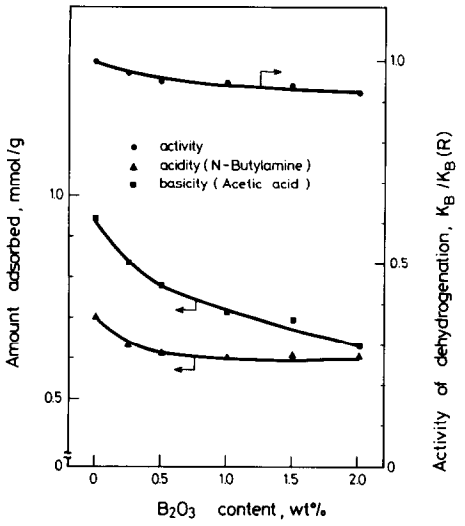

FIG. 11. Effect of doping with B_2O_3 on the activity of dehydrogenation and an adsorbed amount of *N*-butylamine and acetic acid.

and isomerization reactions of cyclohexane. The effects of V_2O_5 molar ratio on the acidic and basic properties, crystal structure, V=O species, and the reaction activities were investigated. The maximum activities of both reactions were observed at the V_2O_5 molar ratio of 0.1 when the calcination temperature was 600°C. That correlated well with surface acidic sites. The incorporation of V_2O_5 into TiO_2ZrO_2 (1/1) not only induces the formation of crystalline $ZrTiO_4$ at a lower temperature, but also enhances the crystalline intensity. Moreover, the higher acidity of ternary oxides with a V_2O_5 molar ratio above 0.25 is due to a phase separation of V_2O_5 and $ZrTiO_4$. Based on the results of poisoning with K_2O and B_2O_3, we propose a stepwise mechanism in which the abstraction of one hydride ion by acidic sites is the rate-determining step, whereas the removal of one proton by basic sites is a fast step.

ACKNOWLEDGMENTS

The authors thank CTCI/Catalyst Research Center for surface area and pore size distribution measurements. This work was supported by Chinese Petroleum Corp.

REFERENCES

1. Balandin, A. A., *Adv. Catal.* **10,** 114 (1958).
2. Carra, S., and Forni, L., *Catal. Rev.* **5,** 159 (1972).
3. Block, J. H., "4th Int. Congr. on Catalysis, Moscow, 1968."
4. Maatman, R., Mahaffy, P., Hoekstra, P., and Addink, C., *J. Catal.* **23,** 105 (1971).
5. Hishida, T., Uchijima, T., Yeneda, Y., *J. Catal.* **17,** 287 (1970).
6. Gland, J. L., Baron, K., and Somorjai, G. A., *J. Catal.* **36,** 305 (1975).
7. Haro, I., Gomez, R., and Ferreira, J. M., *J. Catal.* **45,** 326 (1976).
8. Ruiz-vizczyz, M. E., Novaro, O., Ferreira, J. M., and Gomez, R., *J. Catal.* **52,** 108 (1978).
9. Richardson, P. C., and Rossington, D. R., *J. Catal.* **14,** 175 (1969).
10. Wang, I., Chang, W. F., Shiau, R. J., Wu, J. C., and Chung, C. S., *J. Catal.* **83,** 428 (1983).
11. Wang, I., Wu, J. C., and Chung, C. S., *Appl. Catal.* **16,** 89 (1985).
12. Wu, J. C., Chung, C. S., Ay, C. L., and Wang, I., *J. Catal.* **87,** 98 (1984).
13. Ai, M., *Bull. Chem. Soc. Japan* **49,** 1328 (1976).
14. Johnson, O., *J. Phys. Chem.* **59,** 827 (1955).
15. Miale, J. N., Chen, N. Y., and Weisz, P. B., *J. Catal.* **6,** 278 (1966).
16. Wang, I., Chen, T. J., Chao, K. J., and Tsai, T. C., *J. Catal.* **60,** 140 (1979).
17. Lostaglio, V. J., and Carruthers, J. D., *Chem. Eng. Prog.* March, 46 (1986).
18. Powder diffraction file, Inorganic, No. 7-290 and 9-387.
19. Rubinstein, A. M., Dulov, A. A., and Slinkin, A. A., *J. Catal.* **35,** 80 (1974).
20. Inomata, M., Miyamoto, A., Ui, T., Kobayashi, K., and Murakami, Y., *Ind. Eng. Chem. Prod. Res. Dev.* **21,** 424 (1982).
21. Inomata, M., Miyamoto, A., and Murakami, Y., *J. Catal.* **62,** 140 (1980).
22. Inomata, M., Mori, K., Miyamoto, A., Ui, T., and Murakami, Y., *J. Phys. Chem.* **87,** 754 (1983).
23. Damon, J. P., Bonnier, J. M., and Delmon, B., *Bull. Soc. Chim. France* 449 (1975).
24. Chow, M., Park, S. H., and Sachtler, W. M. H., *Appl. Catal.* **19,** 349 (1985).
25. Pines, H., and Haag, W., *J. Amer. Chem. Soc.* **82,** 2471 (1960).